Exp.-Nr. A2-15/09
Eingang:
an PAC:

Mainz Microtron MAMI

Collaboration A2: "Tagged Photons"
Spokesperson: A. Thomas

Proposal for an Experiment

"Neutron skin evolution in isotopes of Tin and Calcium from coherent pion photoproduction"

Collaborators :

CrystalBall@MAMI collaboration

Spokespersons for the Experiment :
Dan Watts (University of Edinburgh), Douglas MacGregor (University of Glasgow), M Ostrick (Mainz), A Starostin (UCLA)

Abstract of Physics :

The coherent (γ, π^0) reaction can be used to obtain information on the matter form factor of the nucleus. It is proposed to make measurements of four spin zero nuclei in isotopic chains of Calcium and Tin. The central aim of the experiment is to assess the development of a neutron skin with mass number to challenge the descriptions of neutron skin development in modern relativistic mean field and Skyrme Hartree-Fock nuclear theories. The incoherent (γ, π) process exploiting nuclear decay gamma detection will also be studied.

Abstract of Equipment :

The Glasgow-Mainz tagged photon spectrometer will be used with a 885 MeV energy beam from MAMI. The Crystal Ball detector with TAPS as forward wall detector will be used to detect the photons from π^0 decays. The wire chambers will be used to give accurate determination of the target position with respect to the Crystal Ball

MAMI-Specifications :

beam energy	885 MeV
beam current	< 100 nA
beam polarisation	unpolarized

Experiment–Specifications :

experimental hall/beam	A2
photon beam polarisation	unpolarized
detector	Crystal Ball, TAPS, MWPC, PID
target	~ 0.5 mm thickness solid targets

Beam Time Request :

set–up/tests with beam	24 hours
data taking	900 hours

List of participating authors:

- **Institut für Physik, University of Basel, Switzerland**
  I. Jaegle, I. Keshelashvili, B. Krusche, Y. Maghrbi, F. Pheron, T. Rostomyan, D. Werthmüller
- **Institut für Experimentalphysik, University of Bochum, Germany**
  W. Meyer, G. Reicherz
- **Helmholtz–Institut für Strahlen- und Kernphysik, University of Bonn, Germany**
  R. Beck, A. Nikolaev
- **Massachusetts Institute of Technology , Cambridge, USA**
  A. Bernstein, W. Deconinck
- **JINR, Dubna, Russia**
  N. Borisov, A. Lazarev, A. Neganov, Yu.A. Usov
- **School of Physics, University of Edinburgh, UK**
  D. Branford, D.I. Glazier, T. Jude, M. Sikora, D.P. Watts
- **Petersburg Nuclear Physics Institute, Gatchina, Russia**
  V. Bekrenev, S. Kruglov, A. Koulbardis
- **Department of Physics and Astronomy, University of Glasgow, UK**
  J.R.M. Annand, D. Hamilton, D. Howdle, K. Livingston, J. Mancell, J.C. McGeorge, I.J.D. MacGregor, E.F. McNicoll, R.O. Owens, J. Robinson, G. Rosner
- **Department of Astronomy and Physics, Saint Mary's University Halifax, Canada**
  A.J. Sarty
- **Kent State University, Kent, USA**
  D.M. Manley
- **University of California, Los Angeles, USA**
  B.M.K. Nefkens, S. Prakhov, A. Starostin, I.M. Suarez
- **MAX-lab, University of Lund, Sweden**
  L. Isaksson
- **Institut für Kernphysik, University of Mainz, Germany**
  P. Aguar-Bartolome, H.J. Arends, S. Bender, A. Denig, E.J. Downie, N. Frömmgen, E. Heid, O. Jahn, H. Ortega, M. Ostrick, B.Oussena, P.B. Otte, S. Schumann, A. Thomas, M. Unverzagt
- **Institut für Physik, University of Mainz, D**
  J.Krimmer, W.Heil
- **University of Massachusetts, Amherst, USA**
  P.Martel, R.Miskimen
- **Institute for Nuclear Research, Moscow, Russia**
  G. Gurevic, R. Kondratiev, V. Lisin, A. Polonski
- **Lebedev Physical Institute, Moscow, Russia**
  S.N. Cherepnya, L.V. Fil kov, V.L. Kashevarov
- **INFN Sezione di Pavia, Pavia, Italy**
  A. Braghieri, A. Mushkarenkov, P. Pedroni
- **Department of Physics, University of Regina, Canada**
  G.M. Huber
- **Mount Allison University, Sackville, Canada**
  D. Hornidge
- **Tomsk Polytechnic University, Tomsk, Russia**
  A. Fix

- **Physikalisches Institut, University of Tübingen, Germany**
  P. Grabmayr, T. Hehl, D.G. Middleton
- **George Washington University, Washington, USA**
  W. Briscoe, T. Morrison, B.Oussena, B. Taddesse, M. Taragin
- **Catholic University, Washington, USA**
  D. Sober
- **Rudjer Boskovic Institute, Zagreb, Croatia**
  M. Korolija, D. Mekterovic, S. Micanovic, I. Supek

1 Introduction

The coherent (γ, π^0) reaction can be used to obtain information on the matter form factor of the nucleus and can achieve sensitivities sufficient to characterise the neutron skin of stable nuclei. It is proposed to make measurements of four spin zero nuclei in isotopic chains of Calcium and Tin over the photon energy range from threshold to 350 MeV. The central aim of the experiment is to confirm the recent observation of a neutron skin in a heavy beta stable nucleus and to assess the development of a neutron skin with mass number. The incoherent (γ, π^0) reaction will also be studied, exploiting nuclear decay gamma detection capability illustrated with previous Crystal Ball measurements [5].

1.1 The need for accurate neutron skin measurements

The neutron skin thickness of a nucleus is defined by $S = R_n - R_p$ where R_n and R_p are the rms radii for point neutrons and point protons respectively. The need for accurate determination of the neutron skins of stable nuclei comes from a variety of fields in physics. Modern nuclear theories based on Skyrme Hartree Fock (SHF) approaches or relativistic mean field bases (RMF) tend to predict different values for the neutron skin. For example heavy nuclei are predicted to have smaller skins by SHF approaches than for RMF. Recent calculations suggest the neutron and proton rms radii differ by $\sim$0.1 – 0.25 fm for a typical heavy nucleus[9].

The size of the neutron skin for a heavy stable nucleus has direct consequences for poorly established parameters in the neutron rich equation of state. In particular the characteristics of the neutron skin are sensitive to the density dependence of the asymmetry term in neutron rich matter. Obtaining a better constraint on this particularly poorly established quantity is also a high profile aim at Jefferson lab[7] and the proposed FAIR[8] facility.

The need for skin measurements has added impetus because the current uncertainty in the density dependence of the asymmetry term has direct implications for our understanding of neutron star physics. For example the skin thickness of a heavy nucleus has been shown to constrain the mass radii relationship of low mass neutron stars [16], establish the feasibility of direct URCA cooling mechanisms in neutron stars [17], give information on the critical density for the transition between liquid and solid phase [18] and to constrain gravitational wave emission [19]. The neutron skin is also one of the largest systematic uncertainties in low energy tests of the standard model via atomic parity non conservation experiments [2].

Previous measurement of the coherent pion photoproduction reaction for ^{208}Pb using the Crystal Ball at MAMI has shown sensitivity to the neutron skin (results are discussed in section 2.2). This is a result with important consequences for both nuclear and astrophysics and we wish to repeat the skin determination for another heavy nucleus to confirm the observation. A recent letter highlights how multiple measurements of skins across the mass chart using the same experimental technique would put more stringent constrains on the nuclear equation of state than measurements for a single nucleus [3].

The natural candidates for study are the nearest nuclei with closed shells such as the tin (Z=50) and calcium (Z=20) isotopes. Additionally we will extend the scope of the measurements to accurately determine how the neutron skin develops along the isotopic chain to test the theoretical understanding of the skin formation process. Recent calculations[2, 6] show the neutron skin changes from $\sim$-0.05 – 0.1 fm and from $\sim$ -0.0 – 0.15 fm when going from ^{40}Ca to ^{48}Ca and ^{112}Sn to ^{124}Sn respectively. The proposed experiment will be sensitive enough to measure these changes.

1.2 Other techniques employed in neutron skin measurements

1.2.1 Neutron skin measurements with strongly interacting probes

Although sensitivity to neutron skins with strongly interacting probes have been claimed, the interpretation of the data has been shown to be problematic due to many-body strong interaction effects which are difficult to quantify. Recent work which looks in detail at fitting proton scattering data with different skin thicknesses indicate that proton scattering data is not sufficently sensitive to the existence or size of a neutron skin[14].
Work involving heavy ion reactions has also been carried out but the interpretation depends sensitively on the model used to analyse the data [15].

1.2.2 Neutron skin measurements from giant and pygmy resonance studies

There are some recent attempts at neutron skin measurements from observing the character of giant and pygmy resonance modes of nuclei[13]. These data are valuable but implicitly have model dependence in their interpretation as discussed in the references. These studies are an active planned programme for the future FAIR facility. The direct measurements of the skin proposed here would have different and smaller expected model dependencies and therefore provide a valuable test of the systematic error in these studies.

1.2.3 Neutron skin measurements from parity violating electron scattering

There is a PAC A rated experiment expected to run this year in Jefferson Lab [7] which will use parity violating electron scattering for ^{208}Pb at low Q^2 and exploit the large neutron coupling in this kinematic regime to measure the neutron radial form factor at a single value of momentum transfer. The measurement is expected to achieve an accuracy in the skin thickness of $\sim$0.05 fm. One limitation is that the analysis requires asssumptions about the radial dependence of the matter distribution, as the parity violating asymmetry will only be measured at one momentum transfer. The wide application of the technique to many nuclei is also limited by the long beamtimes currently necessary to measure the asymmetries with sufficient accuracy (e.g. a 1 month beamtime is requested for the first measurement on ^{208}Pb).

2 The proposed experiment: Neutron skin measurements with coherent pion photoproduction

The measurement of a matter form factor with an electromagnetic probe offers advantages over techniques involving strong probes. For the real photons in the coherent π process the entrance channel of the reaction is close to ideal. The photon probes the whole volume of the nucleus and shadowing effects are negligible. In fact as the photon is uncharged there are not even the Coulomb scattering effects which are significant for electron scattering on heavy nuclei. The reaction amplitude for the π^0 production reaction on the nucleon has closely equal probabilities on both protons and neutrons because of the dominance of isovector Δ excitation.

In the coherent $A_{gs}(\gamma,\pi^0)A_{gs}$ process the reaction amplitudes for π^0 production from all nucleons add coherently so that the cross section is essentially proportional to $A^2F_m^2(q)$, the square of the mass number times the matter form factor. In PWIA the cross section is given by:

$$\frac{d\sigma}{d\Omega} = A^2\frac{q}{k_\gamma}P_3^2|F_m(q)|^2 sin^2(\theta_\pi) \quad (1)$$

where A is the mass number of the nucleus, q is the momentum transfer to the nucleus, $F_m(q)$ is the matter form factor of the nucleus and P_3 is the contributing pion photoproduction ampli-

tude. The momentum transfer in the reaction is given by $\vec{q} = \vec{p_\gamma} - \vec{p_{\pi^0}}$.

More realistically the π^0 will interact on the way out of the nucleus and this must be accounted for in the analysis. The real part of the interaction produces a difference between the momentum of the π^0 inside and outside the nucleus and as a result the (γ, π^0) angular distribution suffers an angular shift. The imaginary part accounts for pions removed from the flux due to absorption processes. As the photon energy increases towards the Δ-resonance region then it becomes important to include a Δ self-energy term in the potential to account for interaction and propagation of the Δ in the medium.

Accurate pion-nucleus potentials accounting for these effects described above, with parameters fitted to the world database of pion-nucleus scattering data are available and have been incorportated into the theoretical calculation of the coherent process[12].

2.1 Earlier measurements of coherent π^0 photoproduction

There are two measurements of the coherent π^0 photoproduction process in the past decade, using the TAPS detector system [4, 11]. Both measurements suffered large systematic effects, attributed to photon shower reconstruction effects arising from the block like segmented detector configuration of TAPS. This produced large angle dependent variation in pion energy determination and detection efficiencies, which although allowing the diffraction pattern in the angular distribution to be observed, limited the possibility to use the data for accurate skin determinations. The shape of the diffraction maxima extracted from the later data showed unphysical shapes for certain kinematic regions and the analysis of the latter data led to unphysical negative skin thicknesses [10].

2.2 Recent Crystal Ball analysis of coherent pion photoproduction from ^{208}Pb data

The recent Crystal Ball coherent pion production dataset is much improved due to the reduction in systematic effects in the reconstruction of the photon shower because of the symmetrical large acceptance detector configuration. The detection efficiency is uniform for much of the pion angular range and a factor 20 larger than previous TAPS measurements. Other systematics such as the target position were also improved with the use of a wire chamber to locate the target to an accuracy of $\sim$0.5mm relative to the detector apparatus.

The assessment of the neutron skin for ^{208}Pb from this first Crystal Ball experiment is under the final stages of analysis. The measured cross sections as a function of momentum transfer to the nucleus and for different incident photon energy bins are presented in Fig. 1. The analysis of the first minima position is shown in Fig. 2 for five different incident E_γ bins. The minima positions are obtained by fitting a Bessel function to the experimental data in the region of the first minima. These minima positions are shown by the black data points and the errors reflect the variation in the resulting minima position when the parameters of the fit are varied i.e. fitted data range. The red data points show the minima positions corrected for the pion-nucleus interaction according to the model of Ref [12]. The shift in q arising from the interaction is obtained by comparing the minima position from the plane wave and the distorted wave theoretical calculations. Consistent results for a skin thickness of $\sim$0.1fm for ^{208}Pb are obtained.

For the lower photon energies the correction due to the π^0-nucleus interaction is smaller than the effect of a $\sim$0.1 fm neutron skin, so the systematic errors in the skin extraction arising from knowlege of the π-nucleus interaction are expected to be correspondingly small. From these analyses it can be seen that the intrinsic position of the first minima can be determined from

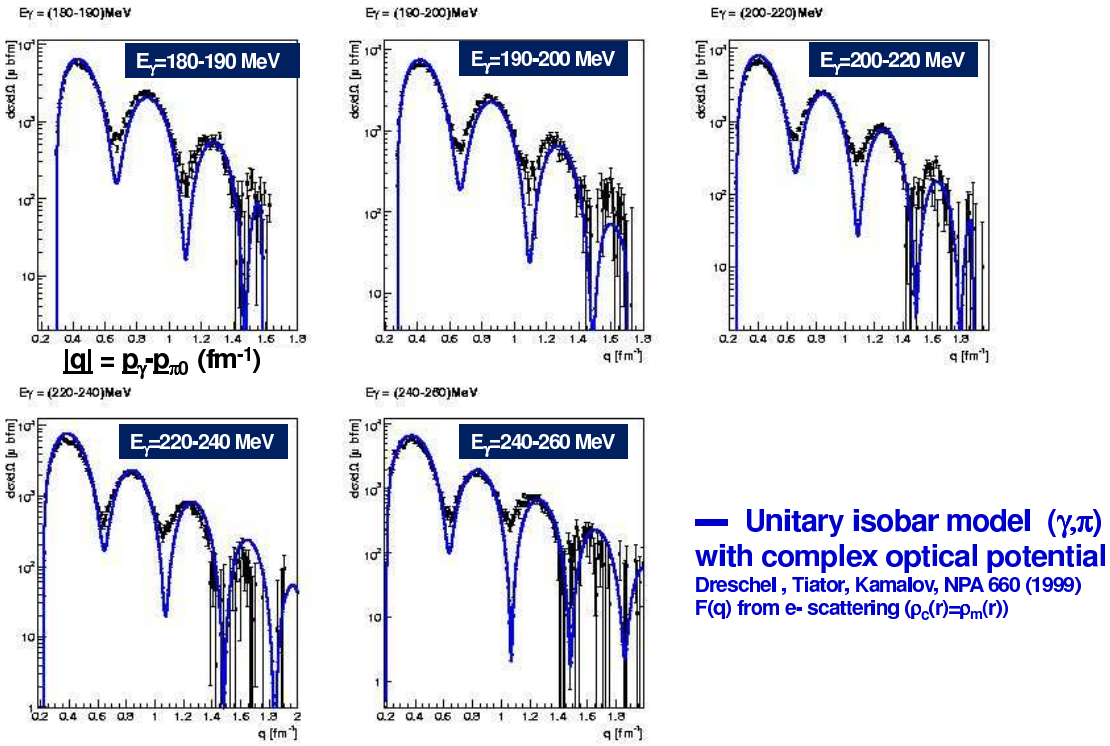

Figure 1: Cross sections as a function of momentum transfer to the nucleus for the $^{208}Pb(\gamma,\pi^0)$ reaction obtained with the Crystal Ball. The solid lines show the predictions of Ref.[12], calculated at the central photon energy in the bin. The caculations have not been passed through the detector acceptance.

the data to an accuracy as small as $\sim$0.002 fm^{-1}, corresponding to a neutron skin thickness sensitivity of $\sim$0.02 fm (see fig 2). The correction to the minima position arising from the π^0-nucleus interaction is only $\sim$0.05 fm at lower photon energies, and the consistency of the first minima position for the corrected data gives confidence in it's treatment by the model.

2.3 The proposed measurement on Tin and Calcium isotopes

As any systematic errors in the magnitude of the minima shift from the π^0-nucleus interaction would be expected to largely cancel for measurements across an isotopic chain, the analysis detailed in the previous section gives an expectation that the intrinsic sensitivity to determining the change in skin thickness across an isotopic chain will be of order $\sim$0.02 fm which is easily sufficient to resolve the changes of order $\sim$0.1-0.15fm predicted by Skyrme HF nuclear models. The count rate estimates for the proposed measurement are extrapolated from the analysis of the ^{208}Pb data described in section 2.2. Similar run conditions for the tagged photon beam, target, PID and wire chamber as for the ^{208}Pb are expected in the proposed experiment. We require the form factor to be determined with a comparable accuracy as for ^{208}Pb, giving a $\sim$20% error in the cross section for a 0.01 fm^{-1} bin in momentum transfer and an incident E_γ bin of $\pm$10 MeV. This will allow similar accuracy in the determination of the minima position as for the ^{208}Pb analysis and give additional information on the shape of the cross section out to the 3rd maxima to give confirmation that the theoretical model is giving a good overall account of the coherent process for these nuclei.

The ^{208}Pb data was obtained with 2.3 days of beam with a tagged photon flux of $\sim 2.5\times10^5\gamma$ sec^{-1}Mev^{-1} on an 0.22×10^{22} nuclei/cm^2 enriched target. It is difficult to obtain isotopically en-

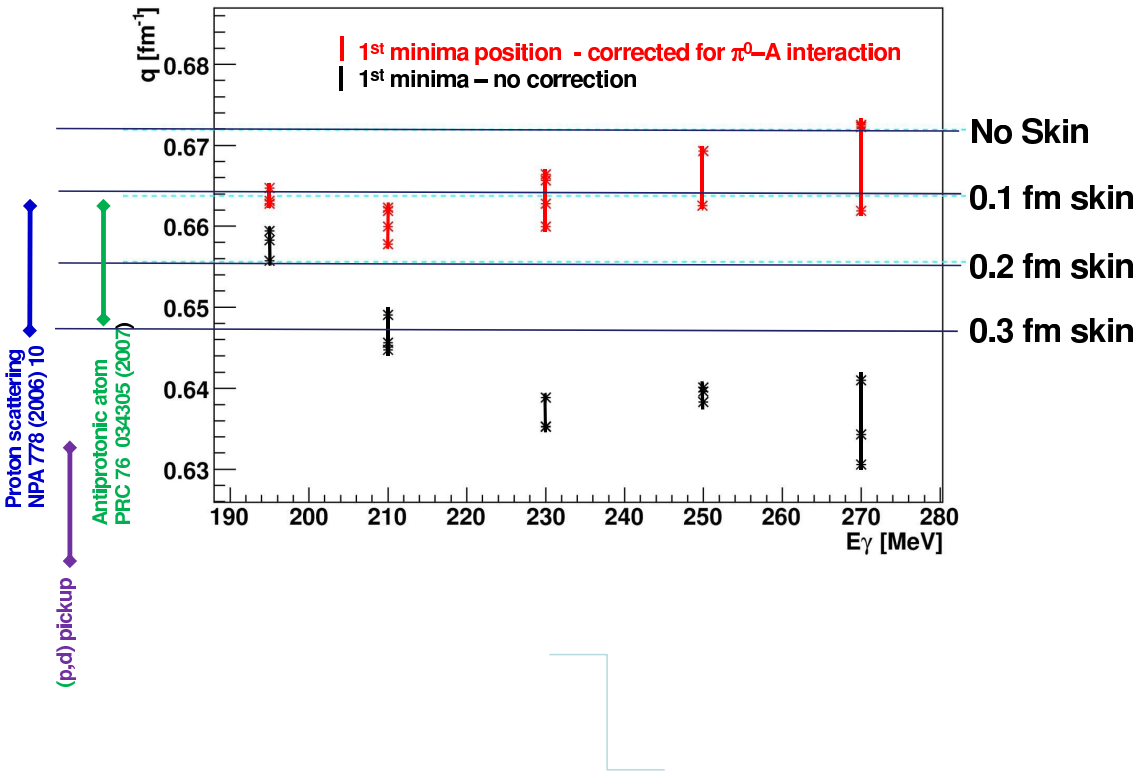

Figure 2: First minima position for $^{208}Pb(\gamma,\pi^0)$ reaction obtained with the Crystal Ball. Black points - uncorrected. Red points - minima position corrected for π^0 distortion. The horizontal lines show the expected momentum transfer for various skin thicknesses. Previous data are shown by the error bars and data points to the left of the figure.

riched targets with thicknesses significantly larger than this so the count rates for the proposed measurement are based on this thickness. Achieving a similar level of measurement accuracy as for ^{208}Pb for the tin and calcium targets requires longer beamtimes due to the A^2 scaling of the coherent cross section (see equation 1).

Therefore to realise the measurement on the three tin isotopes requires $2.3 \times \frac{208^2}{120^2} = 7$ days for each target. Experimental data from the Crystal Ball with a thick natural abundance calcium target is already available to confirm the accuracy of the model, so 1-week measurements will also be sufficient for the two calcium isotopes to establish the 1st minima. The statistical accuracy of the data points in the minima for calcium will be a factor of $\sim$2.5 worse than for ^{208}Pb but will still be sufficient to observe the skin development.
As well as the production running we will require 10% of beamtime with target out measurements (total of 3.5 days). Therefore,
Total beam time request = 38.5 days = 925 hours

References

[1] P. Ring et. al., Nucl. Phys. A624, 349 (1997)

[2] A. Brown et. al., Phys.Rev.C79:035501,2009

[3] M. Centelles et. al., Phys Rev Let. 102 122502 (2009)

[4] Eur.Phys.J.A26:7-18,2005.

[5] C.M. Tarbert et. al., Phys.Rev.Lett. 100 132301 (2008)

[6] J. Dobaczewski, W. Nazarewicz, T. Werner, Z. Phys. A 354, 27-35 (1996)

[7] http://hallaweb.jlab.org/parity/prex/ ; C. Horowitz et. al., Phys. rev. C63 025501 (2005)

[8] http://www.gsi.de/fair

[9] P. Ring et. al., Nucl. Phys. A624, 349 (1997)

[10] B. Krusche *et. al.*, Phys.Lett. B526 287 (2002)

[11] R. Sanderson, Ph.D Thesis, University of Glasgow (2002); L. Fogg, Ph.D Thesis, University of Glasgow (2001)

[12] D. Dreschel, L Tiator, SS Kamalov and Ahin Nan Yang, Nucl. Phys. A660 423(1999)

[13] V. Rodin, Prog Part. Nucl. Phys. 59 issue 1 p268 (2007); J Piekarewicz Phys Rev. C73 044325 (2006)

[14] J. Pekarawicz and S Pieper, Nucl. Phys. A 778 10 (2006)

[15] B-A Li et. al., J. Phys. G Nucl. Part. Phys. 35 (2008) 014044

[16] J. Carriere et al., Astrophys. J. 593 463-471 (2003).

[17] J.M. Lattimer, M. Prakash, The Physics of Neutron Stars, Science 304 536.

[18] C.J. Horowitz, J. Piekarewicz, Phys.Rev.Lett 86 25 (2001).

[19] arxiv: nucl-th 0902.4702 (2009)

3 Experimental apparatus

3.1 Photon Beam

The A2 photon beam is derived from the production of Bremsstrahlung photons during the passage of the MAMI electron beam through a thin radiator. The resulting photons can be circularly polarised, with the application of a polarised electron beam, or linearly polarised, in the case of a crystalline radiator. The degree of polarisation achieved is dependent on the energy of the incident photon beam (E_0) and the energy range of interest, but currently peaks at ∼75% for linear polarisation (Fig. 3) and ∼85% for circular polarisation (Fig. 4). The maximum degree of linear polarisation should be further improved by 5 to 10% by the end of 2009 when the collimation and beam monitoring systems will be optimised for MAMI-C during the installation of the Frozen Spin Target. The Glasgow Photon Tagger (Fig 5) provides energy tagging of the photons by detecting the post-radiating electrons and can determine the photon energy with a resolution of 2 to 4 MeV depending on the incident beam energy, with a single-counter time resolution $\sigma_t = 0.117$ ns [2]. Each counter can operate reliably to a rate of ∼1 MHz, giving a photon flux of $2.5 \cdot 10^5$ photons per MeV. Photons can be tagged in the momentum range from 4.7 to 93.0% of E_0.

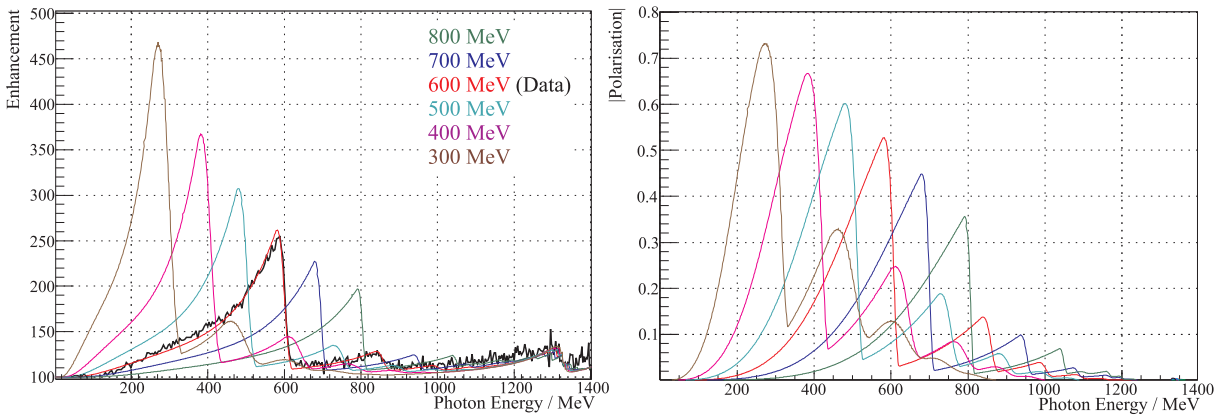

Figure 3: Linear polarisation available with the current collimation system for a variety of crystal orientations. The thin black lines are data obtained during recent MAMI-C runs.

To augment the standard focal plane detector system and make use of the Tagger's intrinsic energy resolution of 0.4 MeV (FWHM), there exists a scintillating fibre detector ('Tagger Microscope') that can improve the energy resolution by a factor of about 6 for a ∼100 MeV wide region of the focal plane (dependent on its position) [4].

3.2 Frozen-Spin Target

Polarisation experiments using high density solid-state targets in combination with tagged photon beams can reach the highest luminosities. For the double polarisation measurements planned with the Crystal Ball detector on polarised protons and deuterons a specially designed, large horizontal ^{3}He/^{4}He dilution refrigerator was built in cooperation with the Joint Institute for Nuclear Research (JINR) Dubna (see Figure 6). It has minimum limitations for the particle detection and fits into the central core of the inner Particle Identification Detector (PID2). This was achieved by using the frozen spin technique with the new concept of placing a thin superconducting holding coil inside the polarisation refrigerator. Longitudinal and transverse polarisations will be possible.
Highest nucleon polarisation in solid-state target materials is obtained by a microwave pumping

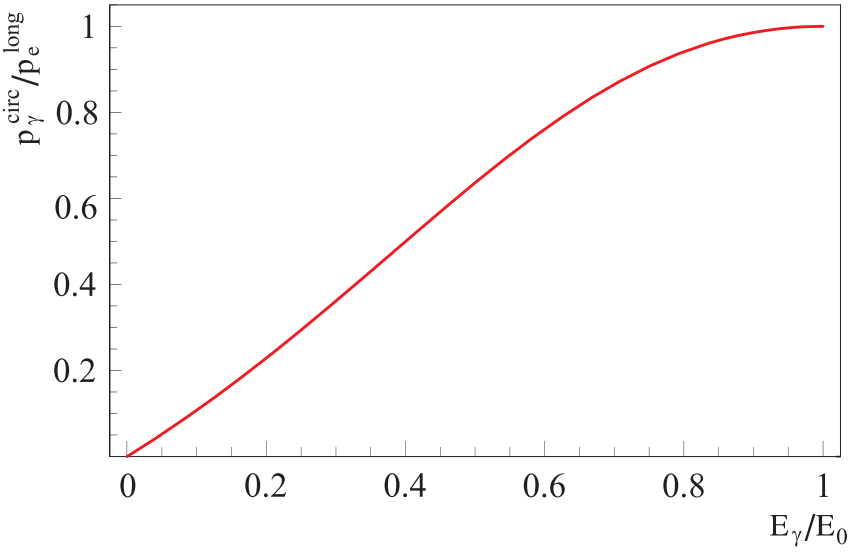

Figure 4: Helicity transfer from the electron to the photon beam as function of the energy transfer. The MAMI beam polarisation is $P_e \approx 85\%$.

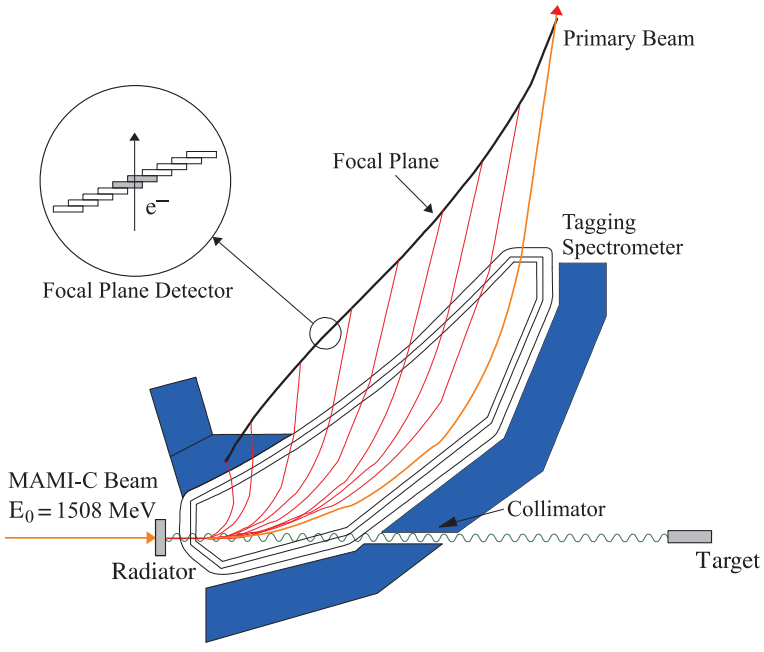

Figure 5: The Glasgow photon tagging spectrometer.

Figure 6: The new dilution refrigerator for the Crystal Ball Frozen Spin Target.

process, known as 'Dynamic Nucleon Polarisation' (DNP). This process is applicable to any nucleus with spin and has already been used in different experiments with polarised proton and deuteron targets. The geometric configuration of the target is the same for the polarised proton and neutron setup. However, since the polarisation measurement of the deuteron is more delicate due to the small size of the polarisation signals, the modification of some basic components is needed. The reason for this is twofold: firstly the magnetic moment of the deuteron is smaller than that of the proton and, in addition, the interaction of the deuteron quadrupole moment with the electric field gradient in the sample broadens the deuteron polarisation signal. An accuracy $\delta P_p/P_p$ of 2 to 3% for the protons and $\delta P_D/P_D$ of 4 to 5% for the deuterons is expected in the polarisation measurement. It has also to be taken into account that the measured deuteron polarisation P_D is not equal to the neutron polarisation P_n. Assuming a 6 % admixture of the D-state of the deuteron, a calculation based on the Clebsch-Gordon coefficients leads to $P_n = 0.91\ P_D$. Several polarised proton and deuteron materials are available such as alcohols and deuterated alcohols (e.g. butanol C_4H_9OH), NH_3, ND_3 or ^{6}LiD. The most important criteria in the choice of material suitable for particle physics experiments are the degree of polarisation P and the ratio k of free polarisable nucleons to the total number of nucleons. Further requirements on polarised target materials are a short polarisation build-up time and a simple, reproducible target preparation. The polarisation resistance against radiation damage is not an issue for experiments with a low intensity tagged photon beam ($\dot{N}_\gamma \approx 5 \cdot 10^7\ \mathrm{s}^{-1}$) as will be used here. However, the limitations of a reduced relaxation time due to overheating of the target beads (Kapitza resistance) will have to be investigated.

Taking all properties together, butanol and deuterated butanol are the best material for this experiment. For protons we expect a maximum polarisation of $P_p = 90\%$ and an average polarisation of $P_p = 70\%$ in the frozen spin mode. Recently, a deuteron polarisation $P_D = 80\%$

was obtained with Trityl doped butanol targets at 2.5 T magnetic field in a ^{3}He/^{4}He dilution refrigerator. At a 0.4 T holding field an average neutron polarisation P_n (see above) of 50 % will be obtained. The filling factor for the ∼2 mm diameter butanol spheres into the 2 cm long, 2 cm diameter target container will be around 60%. The experience from the GDH runs in 1998 [5] shows that, with a total tagged photon flux of $5 \cdot 10^7$, relaxation times of about 200 hours can be expected. The polarisation has to be refreshed by microwave pumping every two days. In conclusion, we estimate that we will achieve the following target parameters:

- Maximum total tagged photon flux in the energy range of 4.7 to 93% of E_0: $\dot{N}_\gamma \approx 5 \cdot 10^7 \mathrm{s}^{-1}$, with relaxation time of 200 hours.
- Target proton density in 2 cm cell: $N_T \approx 9.1 \cdot 10^{22} \mathrm{cm}^{-2}$ (including dilution and filling factors)
- Average proton polarisation $P_p = 70\%$
- Target deuteron density in 2cm cell: $N_T \approx 9.4 \cdot 10^{22} \mathrm{cm}^{-2}$ (including dilution and filling factors)
- Average neutron polarisation $P_n = 50\%$

3.3 Crystal Ball Detector System

The central detector system consists of the Crystal Ball calorimeter combined with a barrel of scintillation counters for particle identification and two coaxial multiwire proportional counters for charged particle tracking. This central system provides position, energy and timing information for both charged and neutral particles in the region between 21° and 159° in the polar angle (θ) and over almost the full azimuthal (ϕ) range. At forward angles, less than 21°, reaction products are detected in the TAPS forward wall. The full, almost hermetic, detector system is shown schematically in Fig. 7 and the measured two-photon invariant mass spectrum is shown in Fig. 8.
The Crystal Ball detector (CB) is a highly segmented 672-element NaI(Tl), self triggering photon spectrometer constructed at SLAC in the 1970's. Each element is a truncated triangular pyramid, 41 cm (15.7 radiation lengths) long. The Crystal Ball has an energy resolution of $\Delta E/E = 0.020 \cdot E[GeV]^{0.36}$, angular resolutions of $\sigma_\theta = 2 \ldots 3°$ and $\sigma_\phi = \sigma_\theta / \sin\theta$ for electromagnetic showers [1]. The readout electronics for the Crystal Ball were completely renewed in 2003, and it now is fully equipped with SADCs which allow for the full sampling of pulse-shape element by element. In normal operation, the onboard summing capacity of these ADCs is used to enable dynamic pedestal subtraction and the provision of pedestal, signal and tail values for each element event-by-event. Each CB element is also newly equipped with multi-hit CATCH TDCs. The readout of the CB is effected in such a way as to allow for flexible triggering algorithms. There is an analogue sum of all ADCs, allowing for a total energy trigger, and also an OR of groups of sixteen crystals to allow for a hit-multiplicity second-level trigger - ideal for use when searching for high multiplicity final states.
In order to distinguish between neutral and charged particles species detected by the Crystal Ball, the system is equipped with PID2, a barrel detector of twenty-four 50 mm long, 4 mm thick scintillators, arranged so that each PID2 scintillator subtends an angle of 15° in ϕ. By matching a hit in the PID2 with a corresponding hit in the CB, it is possible to use the locus of the $\Delta E, E$ combination to identify the particle species (Fig. 9). This is primarily used for the separation of charged pions, electrons and protons. The PID2 covers from 15° to 159° in θ.
The excellent CB position resolution for photons stems from the fact that a given photon triggers several crystals and the energy-weighted mean of their positions locates the photon position to better than the crystal pitch. For charged particles which deposit their energy over only one or

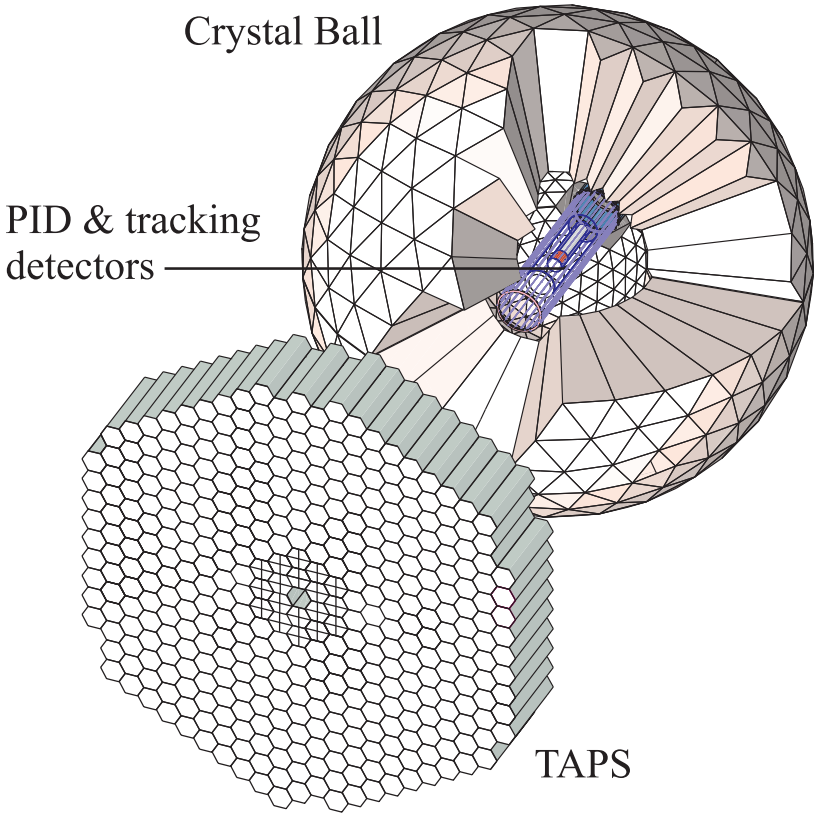

Figure 7: The A2 detector setup: The Crystal Ball calorimeter, with cut-away section showing the inner detectors, and the TAPS forward wall.

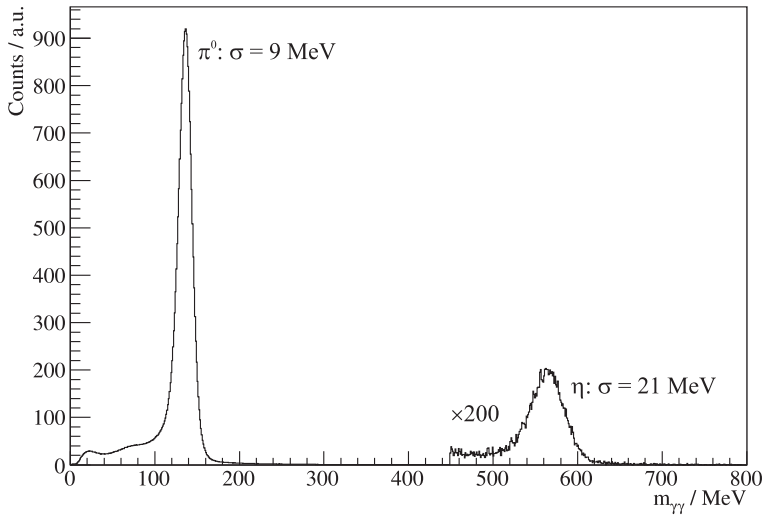

Figure 8: Two photon invariant mass spectrum for the CB/TAPS detector setup. Both η and π^0 mesons can be clearly seen.

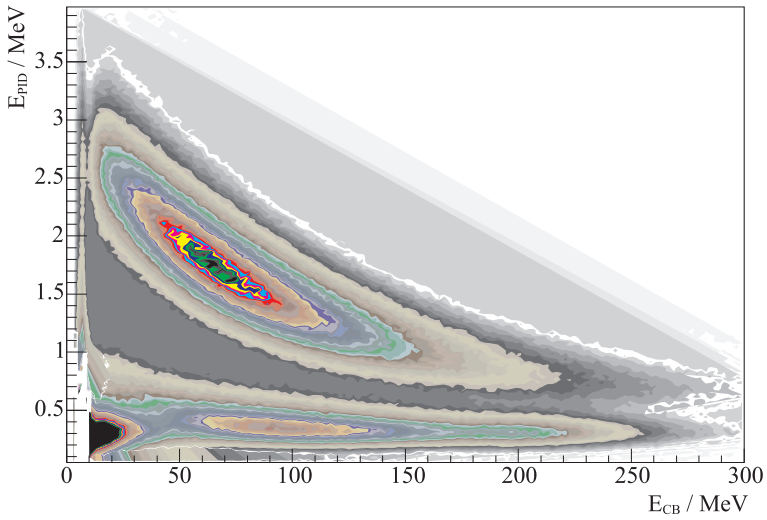

Figure 9: A typical $\Delta E/E$ plot from the Crystal Ball and the PID2 detector. The upper curved region is the proton locus, the lower region contains the pions and the peak towards the origin contains mostly electrons.

two crystals, this is not so precise. Here the tracks of charged particles emitted within the angular and momentum acceptance of the CB detector will be reconstructed from the coordinates of point of intersections of the tracks with two coaxial cylindrical multiwire proportional chambers (MWPCs) with cathode strip readout. These MWPCs are similar to those installed inside the CB during the first round of MAMI-B runs [3]. The most significant difference is that all detector signals are taken at the upstream end of the MWPCs, minimising the material required and facilitating particle detection in the forward polar region.
A mixture of argon (79.5%), ethane (30%) and freon-CF_4 (0.5%) is used as the filling gas. This mixture is a compromise between charge multiplication and localization requirements imposed by the ionizing particle tracks.
Within each chamber both the azimuthal and the longitudinal coordinates of the avalanche will be evaluated from the centroid of the charge distribution induced on the cathode strips. The location of the hit wires(s) will be used to resolve ambiguities which arise from the fact that each pair of inner and outer strip cross each other twice. The expected angular resolution (rms) will be $\sim 2^\circ$ in the polar emission angle θ and $\sim 3^\circ$ in the azimuthal emission angle ϕ.
The MWPCs have been recently installed inside the CB frame and their calibration using both cosmic rays and test beam data is currently underway.

3.4 TAPS Forward Wall

The TAPS forward wall is composed of 384 BaF_2 elements, each 25 cm in length (12 radiation lengths) and hexagonal in cross section, with a diameter of 59 mm. The front of every TAPS element is covered by a 5 mm thick plastic veto scintillator. The single counter time resolution is $\sigma_t = 0.2$ns, the energy resolution can be described by $\Delta E/E = 0.018 + 0.008/E[GeV]^{0.5}$ [1]. The angular resolution in the polar angle is better than 1°, and in the azimuthal angle it improves with increasing θ, being always better than $1/R$ radian, where R is the distance in centimeters from the central point of the TAPS wall surface to the point on the surface where the particle trajectory meets the detector. The TAPS readout was custom built for the beginning of the CB@MAMI program and is effected in such a way as to allow particle identification by Pulse Shape Analysis (PSA), Time Of Flight (TOF) and $\Delta E/E$ methods (using the energy deposit in the plastic scintillator to give ΔE). TAPS can also contribute to the CB multiplicity trigger

and is currrently divided into upto six sectors for this purpose. The 2 inner rings of 18 BaF_2 elements have been replaced recently by 72 $PbWO_4$ crystals each 20 cm in length (22 radiation lengths). The higher granularity improves the rate capability as well as the angular resolution. The crystals are operated at room temperature. The energy resolution for photons is similar to BaF_2 under these conditions [6].

References

[1] S. Prakhov et al.: *Measurement of the Slope Parameter α for the $\eta \to 3\pi^0$ decay with the Crystal Ball dectector at the Mainz Microtron (MAMI-C)*, Phys. Rev. **C 79** (2009) 035204

[2] J.C. McGeorge et al.: *Upgrade of the Glasgow photon tagging spectrometer for Mainz MAMI-C*, Eur. Phys. J. **A 37** (2008) 129

[3] G. Audit et al.: *DAPHNE: a large-acceptance tracking detector for the study of photoreactions at intermediate energies*, Nucl. Instr. Meth. **A 301** (1991) 473

[4] A. Reiter et al.: *A microscope for the Glasgow photon tagging spectrometer in Mainz*, Eur. Phys. J. **A 30** (2006) 461

[5] A. Thomas et al.: *The GDH Experiment at MAMI*, Nucl. Phys. **B 79** (1999) 591

[6] R. Novotny *et al.*: *Scintillators for photon detection at medium energies: A comparative study of BaF-2, CeF-3 and PbWO-4*, Nucl. Instrum. Meth. A **486** (2002) 131